

RESEARCH ARTICLE

## Rotor design optimization of a 4000 rpm permanent magnet synchronous generator using moth flame optimization algorithm

Deniz Perin <sup>a</sup>, Aslan Deniz Karaoglan <sup>b\*</sup>, Kemal Yilmaz <sup>a</sup>

<sup>a</sup> Department of R&D, ISBIR Electric Company, Turkey

<sup>b</sup> Department of Industrial Engineering, Balikesir University, Turkey

gls01@isbirelektrik.com.tr, deniz@balikesir.edu.tr, arg60@isbirelektrik.com.tr

### ARTICLE INFO

#### Article history:

Received: 27 May 2023

Accepted: 23 March 2024

Available Online: 26 March 2024

#### Keywords:

PMSG

Rotor design optimization

Moth flame optimization algorithm

Magnetic flux density distribution

AMS Classification 2010:

13P25, 68T20

### ABSTRACT

The goal of this paper is to optimize the rotor design parameters of 4000 rpm permanent magnet synchronous generator. The factors namely embrace, offset, outer diameter, and magnet thickness are selected as the design parameters those will be optimized in order to hold the magnetic flux density (MFD) distribution and the flux density on stator teeth and stator yoke within a desirable range while maximizing efficiency. The numerical simulations are carried out in the Maxwell environment for this purpose. The mathematical relationships between the responses and the factors are then derived using regression modeling over the simulation data. Following the modeling phase, the moth flame optimization is applied to these regression models to optimize the rotor design parameters. The motivation is determining mathematical relation between the important design parameters of the high speed generator and the measured responses, when standard M530-50A lamination material is used and then to demonstrate the utility of MFO to the readers on this design problem. The optimum factor levels for embrace, offset, outer diameter, and magnet thickness are calculated as 0.68, 30, 161.56, and 8.92 respectively. Additionally, confirmations are done by using Maxwell and the efficiency is calculated as 94.85%, and magnetic distributions are calculated as 1.64, 0.26, and 0.93 Tesla for stator teeth flux density, stator yoke flux density, and MFD; respectively. The results show that the efficiency is maximized and the magnetic distributions are kept within an appropriate range.



### 1. Introduction

Thin (0.20 and 0.35 mm) lamination is often used in high efficiency alternator designs. However, this alternator design significantly increases manufacturing costs. In addition, the availability of this special lamination in the market is limited. It is very difficult to obtain from the market in small quantities, and it is possible to obtain it in case of high purchases in the sector. However, the supply of raw materials for a small amount of production in the sector is a difficult task. The production of high speed alternators with standard materials (eg M530-50A etc. lamination) is the preferred production method, especially in mass production. However, this causes core loss. In this case, alternator design optimization becomes important [1, 2].

There are four different structures in high speed generators: (i) salient-pole generator, (ii)

asynchronous generator (SG), (iii) permanent magnet synchronous generator (PMSG), and (iv) switched reluctance generator. PMSG is the easiest and most common generator type to manufacture. There are many studies on PMSG design optimization in the literature. The related remarkable studies are as follows:

Fang et al. [3] investigated the optimization of SG design. They used double layer interior PMSG (IPMSG). The break angles and length of the PM segments were determined as the factors, while rotor saliency ratio, motor efficiency performance, and back electromotive force (back EMF) are measured as responses. They used finite element analysis (FEA) and the equivalent circuit approach. During the optimization phase, response surface methodology (RSM) is applied. Li and Liu [4] investigated the optimization of the PMSG shape and assessed magnetic field intensity and magnetic flux density

\*Corresponding author

(MFD). Kurt et al. [5] studied on optimizing axial flux PMSG (AFPMSG) design using the Taguchi method. The factors were internal radius, pole number, magnet thickness, and pole utilization factor; and the response was air-gap MFD (AGMFD). They performed optimization using the simplex algorithm, and validated the results using FEA. Hasanien and Muyeen [6] employed genetic algorithm (GA) and RSM to offer an optimum design technique for the controller used in the frequency converter of a variable speed wind turbine (VSWT) driven PMSG. The purpose was to find the best parameters for the PI controllers. Settling time, maximum percentage overshoot (MPOS), maximum percentage undershoot (MPUS), and steady-state error of the voltage profile are the measured responses. The performance of the specified parameters acquired with GA-RSM are then compared to those obtained with a generalized reduced gradient (GRG) approach that takes into account both unsymmetrical and symmetrical errors. Oh et al. [7] conducted research on the design of an IPMSM with concentrated windings. Authors minimized the PM eddy-current loss by moving the magnets at the rotor and keep the MFD in the air gap at a desired range. They used rotor shape and rpm as factors. Several rotor design parameters (bridge size and magnet height) were taken into account in Neubauer et al.'s [8] study. They focused on the IPMSG's rotor design optimization in order to determine their impact on the MFD and machine's performance. A direct-driven surface-mounted PMSG (D-SPMSG)'s magnetic flux linkage optimization was researched by Xie et al. [9]. They used FEA to do simulations and determined winding arrangements, PM specifications and dimensions, as the factors those will be optimized. Demir and Akuner [10] investigated the critical rotor pole data of a line-start PMS motor (LSPMSM). They employed Taguchi for determining factor values of LSPMSM critical rotor pole data in order to optimize efficiency and power factor. They considered the magnet duct dimensions, width of the rib, magnet width, magnet thickness as the factors. Sabioni et al. [11] optimized the design of a 10 kW axial-flux PMSG for direct-coupled wind turbines using non-dominated sorting GA-III (NSGA-III). Material cost, efficiency, outer diameter, and weight are chosen as responses. The authors considered the electromagnetic factors and the dimensions during the design procedure. In order to enhance the design of SPMSG, Dai et al. [12] combined Taguchi and GA. They made an effort to increase efficiency while reducing expense and THD of surface-mounted permanent magnet synchronous machines (SPMSMs). FEA is used to verify the results. They selected the design parameters namely inner radius of rotor, height of air gap, height of magnet, height of stator yoke, width of stator tooth, height of slot, pole-arc to pole-pitch ratio, core length, pole shift angle, magnet eccentricity, magnet segmentation as the factors those have to be

optimized. Gul et al. [13] investigated the DSSR PMSG (dual-stator single-rotor PMSG) optimization. They employed GA to efficiently reduce the cost of the DSSR PMSG and weight. The authors additionally investigated into the MFD distribution. They used power distribution factor, thickness of magnet, axial length, thickness of rotor yoke, thickness of stator yokes, ratio of magnet pole arc to pole pitch as the factors. Semon et al. [14] used RSM for rotor design optimization of a V-type IPMSM to reduce THD while maintaining the desired range of airgap MFD. They used geometrical dimensions of rotor pole shape as the factors. To optimize the THD and voltage regulation rate, Jun et al. [15] explored the design optimization of PMSG for wind power generators using the Taguchi. They tried to determine the optimum factor levels of polar arc coefficient, air gap length, PM thickness, number of turns per phase coil. Karimpour et al. [16] optimized the design of IPMSG using FEA and Taguchi in order to improve efficiency, THD, and the amplitude of induction EMF. They used stator tooth width, stator slot depth, magnet thickness, magnet width, magnet inset, magnet spread angle as the factors. In the following year, Karimpour et al.'s [17] research focused on improving the IPMSG design using FEA and the Taguchi Method. They took into consideration the effects of the magnet inset, magnet thickness, stator tooth width, slot depth, and magnet breadth. The efficiency of the generator, output power, and torque ripple were the measured responses to be optimized. Agrebi et al. [18] employed GA to optimize the design parameters (ratio of the bore radius to the active length of the machine, ratio of the slot depth to the bore radius of the machine, pole pairs number, current surface density, rated power, rated angular rotation speed, induction in the stator yoke, slot number per pole and per phase) of a direct drive PMSG (DDPMSG) for a smart wind turbine, and the results were validated by FEA. Alemi-Rostami et al. [19] investigated the construction of a step-by-step strategy for the design of a PMSG to achieve improved efficiency and power factor while requiring less voltage regulation and PM volume. They employed FEA validation and GA to optimize the design. They determined air gap length, conductor current density, stator slot width, stator slot height, magnet height, magnet width as the factors those have to be optimized. The literature summary is presented in Table 1.

Numerous studies have investigated at the design optimization of PMSG, according to studies that have been published in the literature. The objective of this study is to determine the 16-poled, 3 kVA, 4000 rpm optimum rotor design. In order to do this, we researched the best factors to use while adjusting the rotor's embrace, offset, outer diameter, and magnet thickness in order to maintain the desired range of MFD distribution while increasing efficiency. Maxwell simulations are used to measure the efficiency and distribution of MFD. The mathematical

modeling is done using regression modeling, and the multi-objective optimization is done using the Moth Flame Optimization (MFO) Algorithm.

**Table 1.** Literature summary.

Author(s)	Electric Machine Type	Optimization Method	Responses
Fang et al. [3]	IPMSG	RSM	Rotor saliency ratio, motor efficiency, back EMF
Li and Liu [4]	PMSG	ANSYS Simulations	PMSG shape, magnetic field intensity, MFD.
Kurt et al. [5]	AFPMSG	Taguchi	Air-gap MFD
Hasanien and Muyeen [6]	VSWT driven PMSG	GA, RSM	Settling time, MPOS, MPUS, steady-state error of the voltage profile
Oh et al. [7]	IPMSM	FEA	PM eddy-current loss, air-gap MFD
Neubauer et al. [8]	IPMSG	FEA	MFD inside the PM, voltage, power, maximum power, short circuit current
Xie et al. [9]	D-SPMSG	FEA	Magnetic flux linkage
Demir and Akuner [10]	LSPMSM	Taguchi	Efficiency, power factor
Sabioni et al. [11]	Axial-flux PMSG for direct-coupled wind turbines	NSGA-III	Material cost, efficiency, outer diameter, weight
Dai et al. [12]	SPMSM	Taguchi, GA	Efficiency, cost, THD, MFD
Gul et al. [13]	DSSR PMSG	GA	Cost, weight, MFD
Semon et al. [14]	V-type IPMSM	RSM	THD, air-gap MFD
Jun et al. [15]	PMSG for wind power generators	Taguchi	THD, voltage regulation rate
Karimpour et al. [16]	IPMSG	Taguchi	Efficiency, THD, amplitude of induction EMF
Karimpour et al. [17]	IPMSG	Taguchi	Efficiency, output power, torque ripple
Agrebi et al. [18]	DDPMSG for a smart wind turbine	GA	Mass of the generator's active parts (iron, copper, PMs).
Alemi-Rostami et al. [19]	PMSG	GA	Efficiency, power factor, PM volume

MFO algorithm is a recent and very effective swarm-based optimization technique [20, 21]. MFO is not used for design optimization of PMSGs previously. Using the design parameters namely embrace, offset, outer diameter, and magnet thickness together for optimizing efficiency and magnetic distributions of PMSG by using MFO, is the novelty of this research.

This research's first motivation is determining the relationship between the important design parameters (embrace, offset, outer diameter, and magnet thickness) of the highspeed alternator and the measured responses, when standard M530-50A lamination material is used.

The second motivation is to demonstrate to the readers the utility of MFO with regard to these design problems. As demonstrated by the “No Free Lunch”, none of the offered methods in the literature can handle all difficulties with optimization alone [20, 22]. Therefore, there is always a need to investigate the performance of newly presented algorithms on the presented problems in the literature.

## 2. Mathematical modeling

In this paper, it is aimed to determine the optimum level of the factors (embrace, offset, outer diameter, and magnet thickness) to hold the MFD distribution within a desired range while maximizing the efficiency. To do this, the mathematical relation between these responses and factors have to be calculated in the first stage (then MFO will be run through these models in order to do the optimization). Regression modeling is used to do this. The terms in regression models might be linear, quadratic, or interaction. The models those have these three terms together are referred to as a full quadratic model. The general representation for this type of regression model is given in Eq. (1). This model is used to fit mathematical models to the Maxwell simulations presented in Section 4 [23-26].

$$Y_u = \beta_0 + \sum_{i=1}^n \beta_i X_{iu} + \sum_{i=1}^n \beta_{ii} X_{iu}^2 + \sum_{i < j} \beta_{ij} X_{iu} X_{ju} + e_u \quad (1)$$

$$\beta^T = [\beta_0, \beta_1, \beta_2, \dots, \beta_n] \quad (2)$$

$Y_u$  is the response for  $u$ th run. Responses of this study are the MFD distributions (stator teeth flux density, stator yoke flux density, MFD) and efficiency, which means that in Section 4 four separate regression equations will be calculated.  $X$  terms are the factors ( $X_1$ : embrace,  $X_2$ : offset,  $X_3$ : outer diameter, and  $X_4$ : magnet thickness).  $X_{iu}X_{ju}$  terms represents the interaction terms (in this study maximum 3 interaction terms can be used such as  $X_1X_2$ ,  $X_1X_3$ ,  $X_2X_3$ ).  $e_u$  is the prediction error (PE) for the  $u$ th experimental run [23-26]. The regressin models are calculated by the aid of Minitab Statistical Package in this study. The  $R^2$  (coefficient of determination) calculations and “Analysis of Variance (ANOVA)” are also performed by the aid of Minitab.

$R^2$  is used to assess if the factors included in the mathematical model are adequate to account for the change in response and it is expected to  $R^2$  be nearer to 1 (which means 100 percent). Finally, the significance for each model have to be determined before the performing optimization with MFO algorithm. To do this “Analysis of Variance (ANOVA)” is used. ANOVA is a statistical hypothesis test that use the F-test to measure the significance of a model. ANOVA includes two hypotheses (H0 and H1). H0 indicates that the regression model is insignificant, whereas H1 indicates that it is significant. So, H1 must be true in

order to employ these models during the optimization phase. If the “p-value” (in this study Minitab is used to calculate the P-Value) is lower than the type-I error ( $\alpha$ ) then this means the model is significant (H1 is true) [23-26]. In this study, the confidence level is chosen as 95% (which means  $\alpha=5\%$ ). After completing the modeling, MFO algorithm was utilized for optimization by running through these models [23-26].

### 3. Moth flame optimization (MFO) algorithm

Population based optimization algorithms are widely classified into three main categories: physic-based (such as gravitational search algorithm (GSA), and etc.), evolutionary-based (such as biogeography-based optimization (BBO) algorithm, human evolutionary model, and etc.), and swarm-based (such as artificial bee colony (ABC) algorithm, grey wolf optimizer (GWO) algorithm, and etc.) algorithms.

MFO is a nature-inspired swarm-based meta-heuristic optimization algorithm which is inspired from the moths' navigation mechanism. This mechanism is called transverse orientation. Moths use a very effective method for covering great distances in a straight line at night by maintaining a stable angle with respect to the moon. Because the light source (such as the moon) is far away from the moth, and this ensures that it will fly in a straight line. Regardless of the effectiveness of transverse orientation, moths fly in a spiral around artificial light sources (such as the street lamps and etc.). This is the inefficiency of the transverse orientation and this result in a useless or lethal spiral fly path for moths [20, 21].

In MFO algorithm, the behaviors of the moth-flames are mathematically modeled. In this mathematical model, the candidate solutions are represented by the moths and the factors (input variables) are represented by the positions of the moths (moths can fly in hyper dimensional space). Because of being MFO a population-based algorithm, the set of moths must be represented in a matrix form [20, 21]:

$$M = \begin{bmatrix} m_{1,1} & m_{1,2} & \dots & m_{1,d} \\ m_{2,1} & m_{2,2} & \dots & m_{2,d} \\ \vdots & \vdots & \ddots & \vdots \\ m_{3,1} & m_{3,2} & \dots & m_{n,d} \end{bmatrix} \quad (3)$$

In Eq. (3),  $n$  represents the number of moths and  $d$  represents the number of factors (dimensions). It is also assumed that for each moth, there is an array OM with  $n \times 1$  dimensions for storing the corresponding fitness values (those are the return value of the fitness (objective) function for each moth). Each moth's position vector (for example, the first row in the matrix M) is passed to the fitness function, and the output of the fitness function is assigned to the corresponding moth as its fitness value in the OM matrix (for example the components of OM matrix are:  $OM_1$  for the first row in the matrix M,  $OM_2$  for the second row in the matrix M, and etc.). Flames are another important component of the proposed algorithm. Flames are also represented by a matrix

which has an equal dimension ( $n \times d$ ) with M matrix [20, 21]:

$$F = \begin{bmatrix} F_{1,1} & F_{1,2} & \dots & F_{1,d} \\ F_{2,1} & F_{2,2} & \dots & F_{2,d} \\ \vdots & \vdots & \ddots & \vdots \\ F_{3,1} & F_{3,2} & \dots & F_{n,d} \end{bmatrix} \quad (4)$$

As been at M matrix, it is also assumed that for each flames, there is an array OF with  $n \times 1$  dimensions for storing the corresponding fitness values for the flames where  $n$  is the moths' number. Moths and flames are both solutions, it should be mentioned. The difference is in how we handle and update them at each iteration. Moths are genuine search agents that wander across the search space, whereas flames represent the best moth position obtained thus far. In other terms, flames can be compared to flags or pins dropped by moths when hunting for food. As a result, each moth looks for a flag (flame) and changes it when a better solution is found. With this technique, a moth's optimal answer is never lost [20, 21].

MFO algorithm approximates the global optimal of the optimization problems by using the  $I$ ,  $P$ , and  $T$  functions. The  $I$  function generates a random population of moths (M matrix) and their fitness values (OM array). The main function, the P function, moves the moths around the search space. This function receives the matrix M and eventually returns its updated version. If the termination criterion is satisfied, the T function returns true; otherwise, it returns false (which is represented by  $M=P(M)$  while  $T(M)$  is equal to false). In the  $I$  function, any random distribution may be used [20, 21]:

$$M(i, j) = (ub(i) - lb(i)) * rand() + lb(i) \quad (5)$$

where  $i=1:n$ ,  $j=1:d$ ,  $ub$  and  $lb$  are the upper and lower bounds respectively. Following the  $I$  function's initialization, the  $P$  function (main function) is executed iteratively until the  $T$  function returns true. The  $P$  function moves the moths around the search space inspiring from the transverse orientation. Each moth's position in proximity to a flame is updated using the equation below [20, 21]:

$$M_i = S(M_i, F_j) \quad (6)$$

where  $M_i$  and  $F_j$  are the  $i$ -th moth and  $j$ -th flame.  $S$  is the spiral function which is the moth's primary updating mechanism. The initial point of the spiral must be start from the moth and final point must be the flame's position. The fluctuation should not exceed the search space [20, 21]:

$$S(M_i, F_j) = D_i \cdot e^{bt} \cdot \cos(2\pi t) + F_j \quad (7)$$

In this logarithmic spiral function the spiral flying path of moths is simulated where  $b$  is a constant term that defines the shape of  $S$ ,  $D_i$  is the absolute distance of the  $i$ -th moth for the  $j$ -th flame ( $|F_j - M_i|$ ), and  $t$  is a random number between  $[-1, 1]$ . The  $t$  in the equation defines how close the next position of the moth should be to the flame (where  $t=1$  is the furthest and  $t=-1$  is the closest). By changing  $t$ , a moth can converge on any point in the vicinity of the flame. The

moth's next position would be within a hyper ellipse, which may be assumed in all directions around the flame as a result. Because it governs how moths update their positions around flames, the spiral movement is the most important component of the proposed method. Because of the spiral equation, a moth can fly "around" a flame rather than in the space between them. As a result, the exploration and exploitation of the search space can be ensured. The spiral equation enables a moth to fly "around" a flame rather than in the space between them. As a result, the exploration and exploitation of the search space can be ensured. The position updating guarantees the exploitation around the flames. To increase the likelihood of finding better solutions, the best solutions obtained thus far are referred to as flames. As a result, the matrix F always contains the n most recent best solutions obtained thus far. During optimization, the moths must update their positions in relation to this matrix. To emphasize exploitation, it is assumed that  $t$  is a random number in the range  $[r; 1]$ , with  $r$  decreasing linearly from -1 to -2 over the course of the iteration. It is worth noting that  $r$  is referred to as the convergence constant. Moths using this method tend to exploit their corresponding flames more precisely proportional to the number of iterations. Another issue to consider is that the position updating of moths in relation to  $n$  different locations in the search space may impair the exploitation of the most promising solutions. An adaptive system for the number of flames is suggested to address this issue [20, 21]:

$$flame\ no = round\left(N - 1 * \frac{N-1}{T}\right) \quad (8)$$

where  $l$  is the current iteration count,  $N$  denotes the maximum number of flames, and  $T$  denotes the total number of iterations. The pseudocode for  $P$  function is as follows [20, 21]:

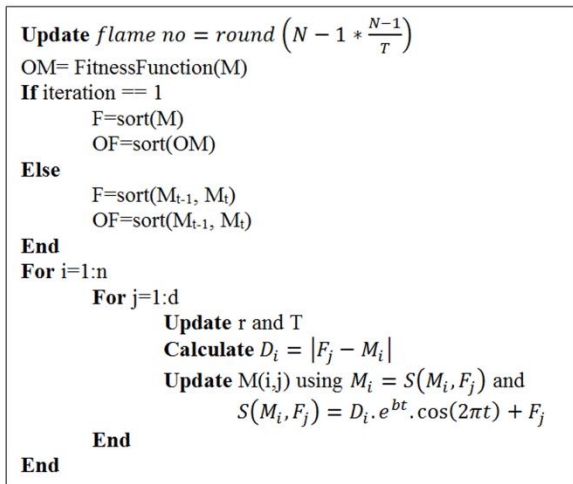


Figure 1. Pseudo code for MFO

Until the  $T$  function returns true, the  $P$  function is executed. The best moth is returned as the best attainable approximation of the optimum when the  $P$

function is terminated.

#### 4. Results and discussions

In this paper, we studied on a 16-poled 4000 rpm 3 kVA PMSG. This PMSG is designed in the Maxwell environment. Some important design parameters of this PMSG are presented in Table 2. The PMSG has a rated power factor of 0.8. All winding material in the Maxwell design is ordinary copper. For lamination, M530-50A Si-Fe is employed. Finally, an H-Class insulating material is chosen. The goal of the first step is to use regression modeling to discover the mathematical relationship between the parameters (embrace ( $X_1$ ), offset ( $X_2$ ), outer diameter ( $X_3$ ), magnet thickness ( $X_4$ )) and the responses (stator teeth flux density ( $Y_1$ ), stator yoke flux density ( $Y_2$ ), MFD ( $Y_3$ ), and efficiency ( $Y_4$ )). An experiment is designed to carry out this phase.

Table 2. Basic design specifications for a 3 kVA PMSG.

Name	Value	Unit	Description	Part
Length	65	mm	Length of core	Stator
Inner Ø of Stator	90	mm	Core diameter (gap side)	Stator
Slot Type	3	N/A	Circular (slot type: 1 to 6)	Stator
Skew Width	1	units	Range number of slot	Stator
Slots	36	units	Number of slots	Stator
Hs0	0.5	mm	Slot opening height	Stator
Bs0	2.5	mm	Slot opening width	Stator
Hs2	14.95	mm	Slot height	Stator
Bs1	4	mm	Slot width	Stator
Bs2	6.27	mm	Slot width	Stator
Rs	1.5	mm	Slot bottom radius	Stator
Inner Ø of Rotor	89	mm	Core diameter (gap side)	Rotor
Length	65	mm	Core length	Rotor
Poles	16	-	Number of poles	Rotor

The flowchart for the mathematical modeling and optimization phase is presented in Figure 2.

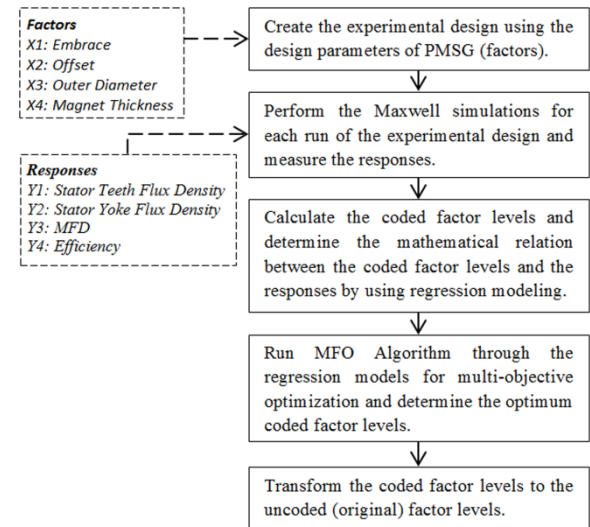


Figure 2. Flowchart for the mathematical modeling and optimization phase.

Table 3 shows the factor levels for this experimental design. Regression models will be generated for both

factor levels with coded and uncoded versions. During the optimization phase, we actually require the coded model. However, in order to demonstrate the true mathematical relationship to the readers, the original models with uncoded factor values are also generated. As a result, uncoded and coded factor levels are presented jointly in Table 4. The experiment has been planned. Eq. (9) is used to code the data.

**Table 3.** Factor levels.

Factors	Sym.	Unit	Levels		
			1	2	3
Embrace	$X_1$	-	0.196	0.588	0.98
Offset	$X_2$	-	10	20	30
Outer Diameter	$X_3$	mm	135	150	165
Magnet Thickness	$X_4$	mm	2	6	10

$$X_{coded} = \frac{X_{uncoded} - ((X_{max} + X_{min})/2)}{((X_{max} - X_{min})/2)} \quad (9)$$

Maxwell simulations are used to execute 25 experimental runs, and the results are shown in Table 4. The disadvantage of manufacturing real PMSG prototypes - which is not appropriate due to expenses - is avoided.

**Table 4.** Maxwell simulations.

Run	Factors (uncoded levels)				Factors (coded levels)			
	$X_{i1}$	$X_{i2}$	$X_{i3}$	$X_{i4}$	$X_{i1}$	$X_{i2}$	$X_{i3}$	$X_{i4}$
1	0.196	10	135	2	-1	-1	-1	-1
2	0.196	10	165	2	-1	-1	1	-1
3	0.98	10	135	2	1	-1	-1	-1
4	0.98	10	165	2	1	-1	1	-1
5	0.196	30	135	2	-1	1	-1	-1
6	0.196	30	165	2	-1	1	1	-1
7	0.98	30	135	2	1	1	-1	-1
8	0.98	30	165	2	1	1	1	-1
9	0.196	10	135	10	-1	-1	-1	1
10	0.196	10	165	10	-1	-1	1	1
11	0.98	10	135	10	1	-1	-1	1
12	0.98	10	165	10	1	-1	1	1
13	0.196	30	135	10	-1	1	-1	1
14	0.196	30	165	10	-1	1	1	1
15	0.98	30	135	10	1	1	-1	1
16	0.98	30	165	10	1	1	1	1
17	0.588	20	135	6	0	0	-1	0
18	0.588	20	165	6	0	0	1	0
19	0.196	20	150	6	-1	0	0	0
20	0.98	20	150	6	1	0	0	0
21	0.588	10	150	6	0	-1	0	0
22	0.588	30	150	6	0	1	0	0
23	0.588	20	150	2	0	0	0	-1
24	0.588	20	150	10	0	0	0	1
25	0.588	20	150	6	0	0	0	0

After several preliminary trials, the full quadratic regression models are derived by linear terms & square terms & interaction terms for the responses. Minitab is used for fitting the regression models and performing the significance tests. Eq. (10) and Table 5 shows the general representation of the fitted regression model and the coefficients of the uncoded (original) models, respectively.

**Table 4.** (Continues).

Run	Responses			
	$Y_{i1}$	$Y_{i2}$	$Y_{i3}$	$Y_{i4}$
1	1.390	0.243	0.754	75.950
2	1.396	0.065	0.754	76.150
3	1.434	1.078	0.754	94.597
4	1.435	0.291	0.754	95.405
5	1.402	0.242	0.764	73.093
6	1.403	0.065	0.764	73.295
7	1.435	0.812	0.754	94.796
8	1.435	0.219	0.754	95.248
9	1.544	0.275	0.955	82.404
10	1.544	0.074	0.773	82.525
11	1.636	1.219	0.947	94.227
12	1.636	0.329	0.947	95.236
13	1.520	0.276	0.957	82.178
14	1.520	0.074	0.957	82.303
15	1.636	1.007	0.947	94.152
16	1.636	0.272	0.947	94.838
17	1.637	0.805	0.902	94.375
18	1.637	0.217	0.902	94.811
19	1.522	0.118	0.918	81.813
20	1.637	0.485	0.902	95.190
21	1.637	0.346	0.902	94.825
22	1.637	0.333	0.902	94.695
23	1.435	0.292	0.754	94.486
24	1.636	0.344	0.947	94.764
25	1.637	0.287	0.902	94.759

$$Y_1 = \beta_0 + \beta_1 X_1 + \beta_2 X_2 + \beta_3 X_3 + \beta_4 X_4 + \beta_5 X_1^2 + \beta_6 X_2^2 + \beta_7 X_3^2 + \beta_8 X_4^2 + \beta_9 X_1 X_2 + \beta_{10} X_1 X_3 + \beta_{11} X_1 X_4 + \beta_{12} X_2 X_3 + \beta_{13} X_2 X_4 + \beta_{14} X_3 X_4 \quad (10)$$

**Table 5.** Regression coefficients for the uncoded factor levels.

Coef.	Term	$Y_1$	$Y_2$	$Y_3$	$Y_4$
$\beta_0$	Const.	1.8561875	16.266952	0.444961	-6.084172
$\beta_1$	$X_1$	0.4186154	4.674439	-0.271387	74.32474
$\beta_2$	$X_2$	-0.0022243	-0.015897	-0.007847	0.102591
$\beta_3$	$X_3$	-0.0091662	-0.217367	0.004506	0.880733
$\beta_4$	$X_4$	0.0893993	0.067595	0.083571	1.450213
$\beta_5$	$X_1^2$	-0.3286391	-0.317811	0.019376	-43.91885
$\beta_6$	$X_2^2$	0.0000700	-0.000108	-0.000050	-0.004902
$\beta_7$	$X_3^2$	0.0000311	0.000714	-0.000022	-0.002921
$\beta_8$	$X_4^2$	-0.0059063	-0.002021	-0.003533	-0.039078
$\beta_9$	$X_1 X_2$	0.0004783	-0.009678	-0.003284	0.091342
$\beta_{10}$	$X_1 X_3$	-0.0000638	-0.023884	0.001935	0.024522
$\beta_{11}$	$X_1 X_4$	0.0106824	0.013672	0.006617	-1.296038
$\beta_{12}$	$X_2 X_3$	-0.0000025	0.000145	0.000076	-0.000280
$\beta_{13}$	$X_2 X_4$	-0.0001063	0.000111	0.000259	0.007420
$\beta_{14}$	$X_3 X_4$	-0.0000083	-0.000305	-0.000190	0.000291

\*Coef.: Coefficient, Const.: Constant

Programming MFO and optimization are done in Matlab. In order to use these equations in the Matlab environment for the MFO approach, the models must be constructed for coded factor values that range from -1 to 1. In this manner, the models are made independent of the units, making multi-objective optimization simple. Table 6 provide the regression models for the levels of coded factors.

The regression models for the responses ( $Y_1, Y_2, Y_3,$  and  $Y_4$ ) have  $R^2$  statistics of 99.29%, 98.88%, 93.93%, and 99.28%, respectively. Table 7 displays the regression models' prediction capabilities. The  $\hat{Y}_i$  values in this table represent the projected outcomes from using the coefficients presented in Table 5. For

each response, the prediction error percentage (PE(%)) is also provided.

**Table 6.** Regression coefficients for the coded factor levels.

Coef.	Term	$Y_{1,coded}$	$Y_{2,coded}$	$Y_{3,coded}$	$Y_{4,coded}$
$\beta_0$	Const.	1.631000	0.341288	0.906305	95.180068
$\beta_1$	$X_1$	0.037722	0.237778	0.006111	7.998778
$\beta_2$	$X_2$	-0.001556	-0.034444	0.011444	-0.373389
$\beta_3$	$X_3$	0.000444	-0.241722	-0.010111	0.224389
$\beta_4$	$X_4$	0.085722	0.031278	0.087278	1.644833
$\beta_5$	$X_1^2$	-0.050500	-0.048836	0.002977	-6.748746
$\beta_6$	$X_2^2$	0.007000	-0.010836	-0.005023	-0.490246
$\beta_7$	$X_3^2$	0.007000	0.160664	-0.005023	-0.657246
$\beta_8$	$X_4^2$	-0.094500	-0.032336	-0.056523	-0.625246
$\beta_9$	$X_1X_2$	0.001875	-0.037938	-0.012875	0.358063
$\beta_{10}$	$X_1X_3$	-0.000375	-0.140438	0.011375	0.144187
$\beta_{11}$	$X_1X_4$	0.016750	0.021438	0.010375	-2.032188
$\beta_{12}$	$X_2X_3$	-0.000375	0.021813	0.011375	-0.042063
$\beta_{13}$	$X_2X_4$	-0.004250	0.004438	0.010375	0.296812
$\beta_{14}$	$X_3X_4$	-0.000500	-0.018312	-0.011375	0.017438

\*Coef. : Coefficient, Const.: Constant

**Table 7.** The accuracy of the models' predictions.

Run	Stator Teeth Flux Density			Stator Yoke Flux Density		
	$Y_{i1}$	$\hat{Y}_{i1}$	$PE_{i1}(\%)$	$Y_{i2}$	$\hat{Y}_{i2}$	$PE_{i2}(\%)$
1	1.390	1.391	0.06	0.243	0.268	9.35
2	1.396	1.394	0.13	0.065	0.058	11.14
3	1.434	1.430	0.30	1.078	1.057	1.94
4	1.435	1.432	0.24	0.291	0.286	1.69
5	1.402	1.393	0.63	0.242	0.223	8.74
6	1.403	1.395	0.57	0.065	0.100	35.14
7	1.435	1.440	0.32	0.812	0.860	5.61
8	1.435	1.440	0.35	0.219	0.176	24.32
9	1.544	1.538	0.37	0.275	0.315	12.83
10	1.544	1.540	0.28	0.074	0.033	126.54
11	1.636	1.644	0.50	1.219	1.191	2.38
12	1.636	1.644	0.49	0.329	0.346	4.94
13	1.520	1.524	0.24	0.276	0.288	4.07
14	1.520	1.524	0.23	0.074	0.092	19.70
15	1.636	1.637	0.07	1.007	1.011	0.41
16	1.636	1.635	0.03	0.272	0.254	7.16
17	1.637	1.638	0.03	0.805	0.744	8.25
18	1.637	1.638	0.09	0.217	0.260	16.61
19	1.522	1.543	1.35	0.118	0.055	115.82
20	1.637	1.618	1.16	0.485	0.530	8.53
21	1.637	1.640	0.16	0.346	0.365	5.18
22	1.637	1.636	0.03	0.333	0.296	12.50
23	1.435	1.451	1.09	0.292	0.278	5.16
24	1.636	1.622	0.85	0.344	0.340	1.11
25	1.637	1.631	0.37	0.287	0.341	15.91

ANOVA is used for determining the significance of the model and summarized in Table 8 (confidence level: 95%) and the confirmation test results are given in Table 7. When there are replicates (multiple observations with identical x-values) in the data, Minitab displays the lack-of-fit test. Replicates are considered "pure error" because only random variation can cause differences in observed response values. In this study, the experimental design is conducted without replicates, so lack-of-fit is not observed in the Minitab reports. Instead of lack of fit test, the p-value test results of ANOVA for the mathematical models are presented in Table 8.

**Table 7.** (Continues).

Run	Efficiency					
	$Y_{i3}$	$\hat{Y}_{i3}$	$PE_{i3}(\%)$	$Y_{i4}$	$\hat{Y}_{i4}$	$PE_{i4}(\%)$
1	0.754	0.767	1.73	75.950	75.906	0.06
2	0.754	0.724	4.10	76.150	76.116	0.04
3	0.754	0.762	1.01	94.597	94.964	0.39
4	0.754	0.764	1.34	95.405	95.750	0.36
5	0.764	0.772	1.09	73.093	73.934	1.14
6	0.764	0.775	1.41	73.295	73.975	0.92
7	0.754	0.715	5.40	94.796	94.424	0.39
8	0.754	0.763	1.23	95.248	95.042	0.22
9	0.955	0.923	3.46	82.404	82.632	0.28
10	0.773	0.835	7.38	82.525	82.911	0.47
11	0.947	0.959	1.25	94.227	93.560	0.71
12	0.947	0.916	3.38	95.236	94.417	0.87
13	0.957	0.970	1.31	82.178	81.847	0.40
14	0.957	0.927	3.27	82.303	81.958	0.42
15	0.947	0.954	0.75	94.152	94.208	0.06
16	0.947	0.957	1.01	94.838	94.895	0.06
17	0.902	0.911	1.03	94.375	94.298	0.08
18	0.902	0.891	1.22	94.811	94.747	0.07
19	0.918	0.903	1.64	81.813	80.433	1.72
20	0.902	0.915	1.46	95.190	96.430	1.29
21	0.902	0.890	1.37	94.825	95.063	0.25
22	0.902	0.913	1.18	94.695	94.316	0.40
23	0.754	0.763	1.12	94.486	92.910	1.70
24	0.947	0.937	1.06	94.764	96.200	1.49
25	0.902	0.906	0.48	94.759	95.180	0.44

**Table 8.** Summary for ANOVA results.

Response	F-Value	P-Value	Result
Stator Teeth Flux Density	100.02	0.000	Significant
Stator Yoke Flux Density	63.17	0.000	Significant
MFD	11.05	0.000	Significant
Efficiency	98.31	0.000	Significant

The results of the ANOVA indicates that P-values for each mathematical model is less than 0.05 – which means that the models are significant. Also the confirmation tests are performed and presented in Table 9.

**Table 9.** Confirmation results.

Run	Factors (uncoded levels)				Factors (coded levels)			
	$X_{i1}$	$X_{i2}$	$X_{i3}$	$X_{i4}$	$X_{i1}$	$X_{i2}$	$X_{i3}$	$X_{i4}$
26	0.392	14	140	4	-0.50	-0.60	-0.67	-0.50
27	0.392	24	140	4	-0.50	0.40	-0.67	-0.50
28	0.392	24	140	8	-0.50	0.40	-0.67	0.50
29	0.784	14	140	4	0.50	-0.60	-0.67	-0.50
30	0.784	14	155	4	0.50	-0.60	0.33	-0.50
31	0.784	14	155	8	0.50	-0.60	0.33	0.50
32	0.784	24	155	8	0.50	0.40	0.33	0.50

**Table 9.** (Continues).

Run	Stator Teeth Flux Density			Stator Yoke Flux Density		
	$Y_{i1}$	$\hat{Y}_{i1}$	$PE_{i1}(\%)$	$Y_{i2}$	$\hat{Y}_{i2}$	$PE_{i2}(\%)$
26	1.580	1.542	2.44	0.367	0.387	5.14
27	1.587	1.541	3.00	0.366	0.357	2.57
28	1.624	1.617	0.45	0.379	0.391	3.16
29	1.592	1.571	1.35	0.702	0.730	3.88
30	1.592	1.569	1.45	0.363	0.361	0.58
31	1.646	1.666	1.18	0.377	0.394	4.35
32	1.646	1.661	0.93	0.363	0.352	3.01

**Table 9.** (Continues).

Run	Efficiency					
	MFD	$\hat{Y}_{i3}$	$PE_{i3}(\%)$	$Y_{i4}$	$\hat{Y}_{i4}$	$PE_{i4}(\%)$
$i$	$Y_{i3}$	$\hat{Y}_{i3}$	$PE_{i3}(\%)$	$Y_{i4}$	$\hat{Y}_{i4}$	$PE_{i4}(\%)$
26	0.859	0.848	1.24	92.361	87.846	5.14
27	0.857	0.855	0.28	92.278	87.271	5.74
28	0.932	0.948	1.73	92.509	90.039	2.74
29	0.856	0.850	0.76	95.045	96.550	1.56
30	0.856	0.846	1.23	95.362	97.082	1.77
31	0.923	0.928	0.56	95.201	97.539	2.40
32	0.929	0.943	1.49	95.132	97.577	2.51

The PE(%) results presented in Table 7 indicates that the prediction performance of the mathematical models for the observations those are not used in the modeling phase is good. As conclusion, results indicate that, the regression models provided in Table 5 and Table 6 are significant, according to the findings.

MFO is coded using the Matlab application [20, 21]. After conducting numerous preliminary tests, it is determined to use 30 search agents in the algorithm. There may be up to 100 iterations. Through a series of early experiments, the number of iterations and the number of search agents were determined. In these preliminary studies, several combinations were tested by gradually increasing the maximum number of iterations from 50 to 5000 and the number of search agents from 10 to 100. A constrained continuous optimization problem is used to model the issue. For this reason the models with coded factor levels presented in Table 6 are used and the factors in this model are then optimized using the MFO technique while adhering to the specified restriction. The goal function and the constraint for the factors are given in Eqs. (11) and (12). According to these functions; While the target for stator teeth flux density ( $Y_{1,coded}$ ) and efficiency ( $Y_{4,coded}$ ) are maximization; the target for stator yoke flux density ( $Y_{2,coded}$ ) is minimization. The target for MFD ( $Y_{3,coded}$ ) is 1.5 tesla. Since the stator tooth is the region exposed to the most intense magnetic field, the stator teeth flux density in this region was tried to be minimized and the maximum saturation point of the material was 1.5 Tesla. It is aimed to maximize the magnetic field value (flux density value) in the stator yoke so that the magnetic flux entering the stator through the tooth can stay in the stator and complete the magnetic circuit. The target values for the MFD value are determined by the additive material of the lamination. For M530-50A used in this study, 1-1.5 Tesla value should be reached.

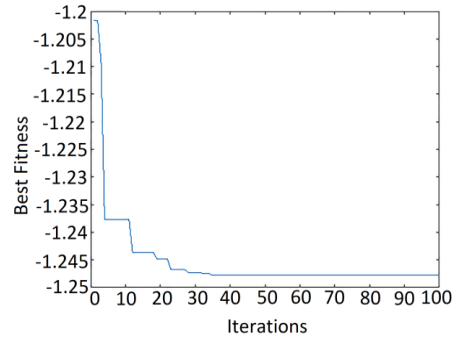
$$Z = |Y_{1,coded}/\max(Y_{i1})| - |Y_{2,coded}/\max(Y_{i2})| - |1.5/\max(Y_{i3}) - Y_{3,coded}/\max(Y_{i3})| + |Y_{4,coded}/\max(Y_{i4})| \quad (11)$$

$$\text{Min } Z \text{ s. t. } X_1 \in [-1,1]; X_2 \in [-1,1]; X_3 \in [-1,1] \quad (12)$$

Keep in mind that the signs provided in the Z equation must be reversed in the Matlab code (see [20, 21, 25,

26] for further information). The CPU time is 5 seconds (on a PC which has 4GB RAM and Intel i5 2.4 GHz processor). In the previous studies published in the literature, the statistical results of the algorithms on multimodal test function are presented by Mirjalili [20] to determine the performance of MFO. Since the multi-modal functions have an exponential number of local solutions, there results show that the MFO algorithm is able to explore the search space extensively and find promising regions of the search space. Results of [20] indicated that the MFO algorithm highly outperforms other well-known algorithms (GA, PSO, and etc.).

Performance index figure that shows the reduction values of the objective function (fitness) during each iteration is presented in Figure 3.

**Figure 3.** Best fitness values in each iteration.

MFO is calculated the optimized factor levels as  $X_1 = 0.68$  (coded value: 0.23),  $X_2 = 30$  (coded value: 1),  $X_3 = 161.56$  (coded value: 0.77), and  $X_4 = 8.92$  (coded value: 0.73). For this optimized factor level combination; the stator teeth flux density is calculated as 1.66 Tesla, stator yoke flux density is calculated as 0.24 Tesla, MFD distribution is calculated as 0.95 Tesla, and efficiency is calculates as 96.43% by MFO algorithm. Maxwell simulations are used for the confirmations and responses are calculated as: stator teeth flux density=1.64 Tesla, stator yoke flux density=0.26 Tesla, MFD=0.93 Tesla, and efficiency=94.85%. Structure of the optimized PMSG, voltage graph of optimized PMSG, and MFD ditributon for the optimized PMSG are displayed in Figures 4-6 respectively. The THD is calculated as 0.21 for the PMSG. The outcomes show that the maximum efficiency has been attained and that the MFD distribution is within acceptable bounds (Figure 6's green zone).

As shown in Figure 6, the slot surface between the rotor and the stator (on the surface of the lamination) is still in the green region from top to bottom. In addition, in the range of 1.4 – 1.6 Tesla, which is between normal and forced zone. Orange zones can be called forced zones. Other colour from orange to red can be called over loaded but in this design we avoided from red zones and stay in max orange zone and do not affect the efficiency.

In general, no negative magnetic flux effect - that will

decrease the efficiency of the optimized PMSG – is observed. Because the red parts are rather minor and the green areas are predominate.

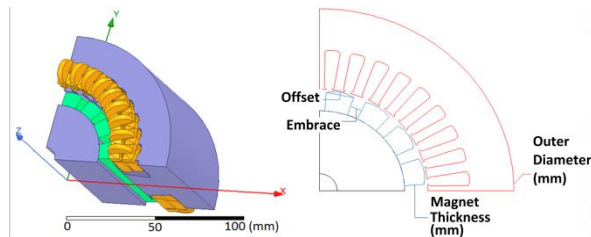


Figure 4. Structure of the optimized PMSG.

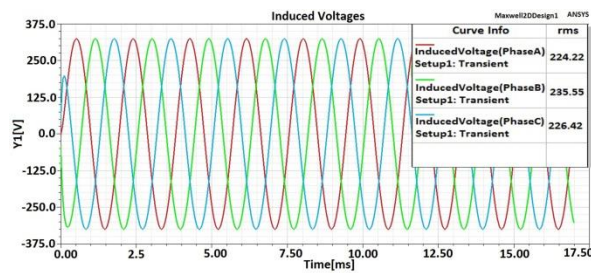


Figure 5. Voltage graph of the optimized PMSG.

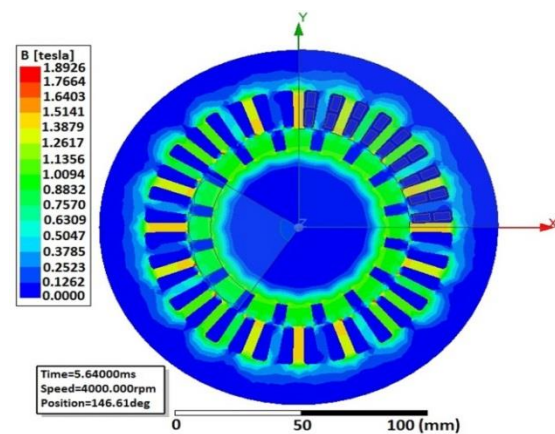


Figure 6. MFD distribution of the optimized PMSG.

The standard lamination (M530-50A) used in this study is normally used in alternators where the magnet structure is thin. In this study, it has been concluded that in the optimized high-speed alternator design, thick magnets should be used in order to achieve the lamination M530-50A saturation and the desired tesla value. In order to use thinner magnets, it is necessary to use more efficient lamination material. The results show that it would be appropriate to use thick magnets in order to obtain the desired Tesla values in high-speed alternators using M530-50A lamination material (the magnet thickness of the unoptimized generator is not specified for commercial confidentiality reasons).

5. Conclusion

In this work, 16-poled, 4000 rpm, 3 kVA PMSG rotor design optimization is carried out. Goal is to optimize the factor levels of embrace, offset, outer diameter (mm), and magnet thickness (mm) for maximizing

efficiency and keeping the magnetic distributions in a desired range. The calculated second order regression equations are fitted to the Maxwell simulation data, and MFO, a successful and recently developed optimization method inspired by nature, is utilized to run through these models. In this study the goal is to show the readers how the MFO algorithm can be used to obtain the desired response values by using the fewest possible experimental runs. Efficiency of the PMSG is maximized to 96.43% and the magnetic distributions are determined as 1.66, 0.24, and 0.95 Tesla for stator teeth flux density, stator yoke flux density, and MFD; respectively. The optimum factor levels for embrace, offset, outer diameter, and magnet thickness are calculated as 0.68, 30, 161.56, and 8.92 respectively. For the optimized factor levels, simulations for confirmation are performed using Maxwell. According to the Maxwell confirmation results: the efficiency is calculated as 94.85%, and magnetic distributions are calculated as 1.64, 0.26, and 0.93 Tesla for stator teeth flux density, stator yoke flux density, and MFD; respectively. Results proved that MFO and regression modeling is effectively used for these type of problems. MFO's striking advantage over previously employed nature-inspired algorithms (such as PSO, GA, and others) is its ability to execute optimization with a relatively low number of iterations (100 for this study). Therefore, we can draw the conclusion that MFO, like the previously discussed nature-inspired algorithms, can be employed successfully for optimization in this field. There is no limitation of MFO and it has only one controllable parameter (that is the number of search agents). So optimization results can not be further improved significantly. Additionally, in the lamination used in the non-optimized stator currently produced by the manufacturer, the thickness of the magnet has been reduced without reducing the useful flux value induced by the magnet in the rotor. This reduced value of 1.08 mm for each magnet corresponds to a total of approximately 17.28 mm for 16 poles considering the total pole in the rotor, which corresponds to two magnets. Compared to the non-optimized PMSG, there was a slight decrease in weight while the size remained the same. This work can be expanded for higher power groups in the future researches. Also the performance of MFO can be compared with the other well-known optimization algorithms in the future researches.

Acknowledgments

We appreciate the Research & Development Department of Isbir Electric Company for allowing us to utilize its resources and software.

References

[1] The company Vacuumschmelze (2021). *Soft Magnetic Cobalt-Iron Alloys Vacoflux and Vacodur* (1st ed.). VACUUMSCHMELZE GmbH & Co. KG, Hanau.  
 [2] Bartolo, J.B., Zhang, H., Gerada, D., De Lillo, L.,

- & Gerada, C. (2013). High speed electrical generators, application, materials and design. *1st IEEE Workshop on Electrical Machines Design, Control and Diagnosis (WEMDCD)*, March 11-12, Paris, France.
- [3] Fang, L., Jung, J.W., Hong, J.P. & Lee, J.H. (2008). Study on high-efficiency performance in interior permanent-magnet synchronous motor with double-layer PM design. *IEEE Transactions on Magnetics*, 44(11), 4393-4396.
- [4] Li, H., & F. Liu (2011). The electromagnetic field analysis of permanent magnet synchronous generator based on ANSYS. *2nd International Conference on Advanced Measurement and Test (AMT 2011)*, Nanchang, PRC, June 24-26, 2011.
- [5] Kurt, U., Onbilgin, G., & Ozgonenel, O. (2012). Defining design criteria of an axial flux permanent magnet synchronous generator. *International Review of Electrical Engineering (IREE)*, 7(1), 3290-3296.
- [6] Hasanien, H.M., & Muyeen, S.M. (2013). A Taguchi approach for optimum design of proportional-integral controllers in cascaded control scheme. *IEEE Transaction on Power Systems*, 28 (2), 1636-1644.
- [7] Oh, S.Y., Cho, S.Y., Han, J.H., Lee, H.J., Ryu, G.H., Kang, D., & Lee, J. Design of IPMSM rotor shape for magnet eddy-current loss reduction. *IEEE Transactions on Magnetics*, 50(2), Article Number: 7020804.
- [8] Neubauer, M., Neudorfer, H., & Schrodli, M. (2016). Influence of the rotor optimization of an interior permanent magnet synchronous generator on the short circuit behavior. *22nd International Conference on Electrical Machines (ICEM)*, 1828-1834, Sep. 04-07, Lausanne, Switzerland.
- [9] Xie, Q., Zhang, Y.B., Yu, Y.A., Si, G.Q., Yang, N.N., & Luo, L.F. (2016). A novel method to magnetic flux linkage optimization of direct-driven surface-mounted permanent magnet synchronous generator based on nonlinear dynamic analysis. *Energies*, 9(7), Article Number: 557.
- [10] Demir, U., & Akuner, M.C. (2017). Using Taguchi method in defining critical rotor pole data of LSPMSM considering the power factor and efficiency. *Tehnicki Vjesnik-Technical Gazette*, 24(2), 347-353.
- [11] Sabioni, C.L., Ribeiro, M.F.O, & Vasconcelos, J.A. (2018). Robust design of an axial-flux permanent magnet synchronous generator based on many-objective optimization approach. *IEEE Transactions on Magnetics*, 54(3), Article Number: 8101704.
- [12] Dai, L., Gao, J., Zhang, W. & Huang, S. (2019). A genetic-Taguchi global design optimization strategy for surface-mounted PM machine. *22nd International Conference on Electrical Machines and Systems (ICEMS)*, pp. 1-6, Harbin, China.
- [13] Gul, W., Gao, Q. & Lenwari, W. (2020). Optimal design of a 5-MW double-stator single-rotor PMSG for offshore direct drive wind turbines. *IEEE Transactions on Industry Applications*, 56(1), 216-225.
- [14] Semon, A., Melcescu, L., Craiu, O. and Crăciunescu, A. (2019). Design optimization of the rotor of a V-type interior permanent magnet synchronous motor using response surface methodology. *11th International Symposium on Advanced Topics in Electrical Engineering (ATEE)*, pp. 1-4, Bucharest, Romania, Mar. 28-30.
- [15] Jun, Z., Guanghua, L., Di, C., & Zhenyi, Z. (2019). Voltage regulation rate and THD optimization analysis of coreless axial flux PM synchronous generator for wind power generation. *IEEE Transactions on Electrical and Electronic Engineering*, 14(10), 1485-1493.
- [16] Karimpour, S.R., Besmi, M.R., & Mirimani, S.M. (2020). Optimal design and verification of interior permanent magnet synchronous generator based on FEA and Taguchi method. *International Transactions on Electrical Energy Systems*, 30(11), Article Number: E12597.
- [17] Karimpour, S.R., Besmi, M.R., & Mirimani, S.M. (2021). Multi-objective optimization design and verification of interior PMSG based on finite element analysis and Taguchi method. *International Journal of Engineering*, 34(9), 2097-2106.
- [18] Agrebi, H.Z., Benhadj, N., Chaieb, M., Sher, F., Amami, R., Neji, R., & Mansfield, N. (2021). Integrated optimal design of permanent magnet synchronous generator for smart wind turbine using genetic algorithm. *Energies*, 14(15), Article Number: 4642.
- [19] Alemi-Rostami, M., Rezazadeh, G., Alipour-Sarabi, R., & Tahami, F. (2022). Design and optimization of a large-scale permanent magnet synchronous generator. *Scientia Iranica*, 29(1), 217-229.
- [20] Mirjalili, S. (2015). Moth-flame optimization algorithm: A novel nature-inspired heuristic paradigm. *Knowledge-Based Systems*, 89, 228-249.
- [21] Mirjalili, S. <https://seyedalimirjalili.com/mfo>. (Access: Apr 04, 2023)
- [22] Wolpert, D.H., & Macready, W.G. (1997). No free lunch theorems for optimization. *IEEE Transactions on Evolutionary Computation*, 1, 67-82.
- [23] Montgomery, D.C. (2013). *Design and analysis of experiments* (8th ed.). John Wiley & Sons, New Jersey, USA.
- [24] Mason, R.L., Gunst, R.F., & Hess, J.L. (2003). *Statistical Design and Analysis of Experiments* (2nd ed.). John Wiley & Sons, New Jersey, USA.
- [25] Ileri, E., Karaoglan, A.D., & Akpinar, S. (2020). Optimizing cetane improver concentration in biodiesel-diesel blend via grey wolf optimizer algorithm. *Fuel*, 273, Article Number:117784.
- [26] Karaoglan, A.D., Perin D. (2022). Rotor Design Optimization of a synchronous generator by considering the damper winding effect to minimize THD using grasshopper optimization algorithm. *An International Journal of Optimization and Control: Theories & Applications (IJOCTA)*, 12(2), 90-98, <https://doi.org/10.11121/ijocta.2022.1181>.

**Deniz Perin** received MSc. and Ph.D. Degrees in Physics from Balikesir University in the years 2008 and 2015 in Turkey, respectively. He has studied magnetic flux leakage (MFL) and magnetic non-destructive testing in Ph.D. and in research program of Cardiff University Wolfson Centre for magnetics. From 2017 till now, he is working on magnetic design & simulations of synchronous generators with ANSYS Maxwell in Isbir Electric Co Research & Development Department as a research and development expert.

 <https://orcid.org/0000-0003-3697-3499>

**Aslan Deniz Karaoglan** received his Industrial Engineering diploma from Gazi University in Turkey in 2001, MSc. from Balikesir University in 2006, and Ph.D. from Dokuz Eylul University in 2010 in Turkey. His research interests are design of experiments, statistical process control, artificial intelligence, and optimization. He is a professor at Balikesir University (Turkey), Department of Industrial Engineering.

 <https://orcid.org/0000-0002-3292-5919>

**Kemal Yilmaz** received the B.S. degree in 2015 from the Department of Mechatronics Engineering - Karabuk University in 2015. Since 2017, he has been working as project and simulation Engineer in Isbir Electric Co Research & Development Department. His research interests are magnetic design and simulations of synchronous generators with Ansys Maxwell.

 <https://orcid.org/0000-0001-5371-4267>

An International Journal of Optimization and Control: Theories & Applications (<http://ijocta.balikesir.edu.tr>)



This work is licensed under a Creative Commons Attribution 4.0 International License. The authors retain ownership of the copyright for their article, but they allow anyone to download, reuse, reprint, modify, distribute, and/or copy articles in IJOCTA, so long as the original authors and source are credited. To see the complete license contents, please visit <http://creativecommons.org/licenses/by/4.0/>.